

# S-BORM: Reliability-based optimization of general systems using buffered optimization and reliability method

Ji-Eun Byun<sup>a,\*</sup>, Welington de Oliveira<sup>b</sup>, Johannes O. Royset<sup>c</sup>

<sup>a</sup>James Watt School of Engineering, University of Glasgow, Glasgow, United Kingdom

<sup>b</sup>Mines Paris, Université PSL, Centre de Mathématiques Appliquées (CMA), Sophia Antipolis, France

<sup>c</sup>Operations Research Department, Naval Postgraduate School, California, United States

---

## Abstract

Reliability-based optimization (RBO) is crucial for identifying optimal risk-informed decisions for designing and operating engineering systems. However, its computation remains challenging as it requires a concurrent task of optimization and reliability analysis. Moreover, computation becomes even more complicated when considering performance of a general system, whose failure event is represented as a link-set of cut-sets. This is because even when component events have smooth and convex limit-state functions, this definition leads to system events with nonsmooth and nonconvex limit-state functions. To address the challenge, this study develops an efficient algorithm to solve RBO problems of general system events. We employ the buffered optimization and reliability method (BORM), which utilizes, instead of the conventional failure probability definition, the buffered failure probability. The proposed algorithm solves a sequence of Difference-of-Convex RBO models iteratively by employing a proximal bundle method. To demonstrate its efficiency, accuracy, and robustness, we present three numerical examples with parametric studies. The examples include complex systems such as a structural system with 108 failure modes and an electrical system with components undergoing reliability growth.

*Keywords:* Reliability-based optimization, data-driven optimization, general systems, buffered failure probability, DC programming, proximal bundle method, superquantile

---

## 1. Introduction

To secure disaster resilience of a community, it is crucial to make optimal decisions when designing and operating engineering systems (e.g., structural systems, infrastructures, and mechanical systems) and these decisions should account appropriately for hazard risks. This can be done by performing reliability-based optimization (RBO), where a design cost is minimized while satisfying reliability constraints [1, 2]. A common, reasonable way to define such reliability constraints is to constrain a failure probability under a

---

\*Corresponding author

*Email address:* Ji-Eun.Byun@glasgow.ac.uk (Ji-Eun Byun)

target level. However, such a combined task of probabilistic analysis and optimization makes RBO problems theoretically and computationally challenging. Moreover, RBO problems become even more challenging when an event of interest is a system event, whose performance is determined by joint performance of multiple component events. Nonetheless, to enable accurate decision-making, it is critical to consider interdependent component events simultaneously [3, 4].

To formulate an RBO problem, a system failure probability needs to be represented as a function of design variables. Since explicit expression of such functions is often unavailable, various approximate methods have been proposed. This includes replacing failure probability by reliability index [5, 6] or failure rate [7], evaluating probabilities approximately using surrogate models such as kriging [8, 9] or co-kriging [10], simplifying optimization by approximate functions [2, 11], and leveraging metaheuristic optimization such as genetic algorithms [12] or particle swarm optimization algorithms [13].

While these previous studies provide characteristic advantages of their own, another promising approach is to directly utilize realizations of random variables, i.e., samples or data points. This strategy exempts us from deriving problem-specific formulas. Moreover, it enables data-driven optimization, which is particularly favored when underlying parametric distributions of given data are unknown. However, the definition of failure probability makes it challenging to handle realizations during optimization. This is because they assign either 1 or 0 depending on whether a sample lies in a failure domain or not. Such binary assignment lacks gradient information. This makes it difficult to employ efficient gradient-based optimization algorithms [14]. Although [15] proposed formulations to calculate such gradients, some restrictive conditions are necessary (e.g., random variables follow the multivariate normal distribution or transformation thereof). The challenge can be addressed by utilizing, instead of the conventional failure probability, the *buffered failure probability* [16, 17, 18, 19]. This way of defining reliability permits (sub)gradient information even in a data-driven setting. Motivated by this fact, [17] proposed the *buffered optimization and reliability method* (BORM), which enables efficient data-driven optimization of reliability. It is noted that the use of the buffered failure probability still preserves the philosophy of risk management by the conventional failure probability as the two failure probabilities have strongly positive correlations [17].

General systems are often represented as a series system of multiple parallel systems or equivalently, a link-set of cut-sets. This representation is useful since it can cover any system types, but also highlights the challenges associated with optimization of general systems: A system event tends to have a nonsmooth and nonconvex limit-state function with respect to design variables even when component events have smooth and convex limit-state functions [16]. This effect is unavoidable, but is made more manageable in BORM because it avoids the 0-1 discontinuity caused by failure probability formulations. Moreover, BORM allows us to bring forward the component limit-state functions, which tend to be smooth as functions of design variables. This enables us to employ an efficient bundle method for the optimization subproblems; see [20, Ch. 10] and [21] for an introduction to convex bundle methods and [22] for the nonconvex proximal bundle

method employed as an auxiliary algorithm in this work.

Motivated by the challenges above, this study proposes a novel algorithm for reliability-based optimization, particularly intended to handle general systems. Since the algorithm addresses *system* reliability optimization using BORM, it is named *S-BORM*. The S-BORM algorithm solves RBO subproblems that are formulated by BORM and uses data or sample points to estimate the buffered failure probability. Such subproblems fall into the class of Difference-of-Convex (DC) optimization [23] and are handled by the DC bundle method of [22]. As we show in the following discussions, the DC representation of RBO subproblems can be derived by linearizing limit-state functions at a current solution candidate. We further enhance computational efficiency by employing an active-set strategy, which significantly reduces the number of samples (or data points) that need to be considered in each iteration. We justify S-BORM by relying on the properties of the DC bundle method, but a formal proof of convergence and rate of convergence is beyond the scope of the paper. Instead, we test the algorithm extensively on three, increasingly complex structures. It is noted that the S-BORM algorithm is also developed as a Matlab-based function, which is available at <https://github.com/jieunbyun/sborm>.

The paper is organized as follows. Section 2 illustrates background theories related to developing the S-BORM algorithm. The algorithm is proposed in Section 3. Performance of the algorithm is thoroughly investigated by three numerical examples in Section 4 and various parametric studies in Section 5. For completeness, the following discussions present both application and mathematical issues. Readers who are not interested in mathematical details of the optimization scheme may skip Sections 2.3, 3.2, and 3.4.

## 2. Background

### 2.1. General system events and reliability-based optimization

A failure event of a general system is represented as a series system of parallel systems of component failure events, or equivalently, a link-set of cut-sets, i.e.,

$$E_{\text{sys}} = \bigcup_{k=1}^K \bigcap_{q \in Q_k} E_q, \quad (1)$$

where  $E_{\text{sys}}$  and  $E_q$  ( $q \in Q_k$ ,  $k = 1, \dots, K$ ) refer to the failure event of a system and component  $q$ , respectively. To determine whether a system or component event  $E$  is either failure or survival, a limit-state function  $g(\mathbf{x}, \mathbf{V})$  can be used to account for performance of the corresponding system or component. The function depends on design variables  $\mathbf{x} = (x_1, \dots, x_D)$  and random vector  $\mathbf{V} = (V_1, \dots, V_M)$ . A corresponding event  $\mathbf{v}$  of  $\mathbf{V}$  is considered a failure if  $g(\mathbf{x}, \mathbf{v}) > 0$  and a survival, otherwise<sup>1</sup>. Thereby, the definition of a system

---

<sup>1</sup>If necessary, one can reverse the definition of failure and survival (i.e., a failure event if  $g(\mathbf{x}, \mathbf{v}) < 0$ ) by reversing the sign of limit-state functions.

failure event in (1) can be represented in terms of limit-state functions as

$$g_{\text{sys}}(\mathbf{x}, \mathbf{v}) = \max_{k=1, \dots, K} \min_{q \in Q_k} g_q(\mathbf{x}, \mathbf{v}), \quad (2)$$

where  $g_{\text{sys}}(\mathbf{x}, \mathbf{v})$  denotes the limit-state function of a system.

The most common formulation of reliability-based optimization is to minimize design cost  $c(\mathbf{x})$  while satisfying a reliability constraint (i.e., system failure probability be less than a target value  $p_f^t$ ):

$$\min_{\mathbf{x} \in \mathbb{X}} \quad c(\mathbf{x}) \quad (3a)$$

$$\text{subject to} \quad p(\mathbf{x}) \leq p_f^t, \quad (3b)$$

where  $\mathbb{X}$  denotes a simple constraint set, and the conventional failure probability is defined as

$$p(\mathbf{x}) = P[g_{\text{sys}}(\mathbf{x}, \mathbf{V}) > 0]. \quad (4)$$

Alternatively, the reliability constraint (3b) can be represented in terms of a quantile:  $p(\mathbf{x}) \leq p_f^t$  if and only if  $q_{1-p_f^t}(\mathbf{x}) \leq 0$ , where  $q_\alpha(\mathbf{x})$  is the  $\alpha$ -quantile of  $g_{\text{sys}}(\mathbf{x}, \mathbf{V})$ . Thus, (3) is equivalent to the problem

$$\min_{\mathbf{x} \in \mathbb{X}} \quad c(\mathbf{x}) \quad (5a)$$

$$\text{subject to} \quad q_{1-p_f^t}(\mathbf{x}) \leq 0. \quad (5b)$$

It is noted that solving (3) and (5) requires an analytical formula of the reliability constraint (3b) and (5b), respectively. However, for general systems, deriving such an analytical representation is usually impossible. Alternatively, the failure probability in (4) can be estimated by realizations of  $\mathbf{V}$  (i.e., samples or data points),  $\mathbf{v}_1, \dots, \mathbf{v}_N$ , i.e.,

$$\hat{p}(\mathbf{x}) = \sum_{n=1}^N p_n \cdot \mathbb{I}[g(\mathbf{x}, \mathbf{v}_n) > 0], \quad (6)$$

where  $\hat{p}(\mathbf{x})$  is the estimated failure probability given  $\mathbf{x}$ , and  $p_n$  is a probability or weight of realization  $\mathbf{v}_n$ <sup>2</sup>. The Heaviside function  $\mathbb{I}[\cdot]$  takes value 1 if the given statement is true and 0, otherwise. When replacing in (3) the probability  $p(\mathbf{x})$  by  $\hat{p}(\mathbf{x})$ , the Heaviside function in (6) greatly complicates computation because it lacks (sub)gradient information. The gradient is not defined when  $g(\mathbf{x}, \mathbf{v}) = 0$  and remains 0 at all other values. One possible remedy for this issue is to approximate  $\mathbb{I}[\cdot]$  with a DC function provided that the limit-state functions have explicit DC decompositions [24]. For more general limit-state functions as in this work, an implementable approach consists of employing the concept of *buffered failure probability*. This is discussed in the following subsection.

---

<sup>2</sup>For example, if  $\mathbf{v}_1, \dots, \mathbf{v}_N$  are generated by Monte Carlo simulation (MCS),  $p_n = 1/N$  for all  $n$ .

## 2.2. Buffered optimization and reliability method

The paper [17] recently proposed a framework of reliability-based optimization, namely *buffered optimization and reliability method* (BORM). Being traced back to [16], BORM replaces the failure probability in (3b) by the buffered failure probability. While details can be found in the references, this section presents a brief illustration that is directly related to the following discussions. Above all, the two failure probabilities are distinguished by how the threshold value of limit-state functions is defined to determine a failure event. According to the conventional probability, this threshold is fixed at 0. In contrast, the buffered probability defines such threshold as a quantile value whose associated superquantile is 0. In more detail, consider a random variable  $Y$  and its CDF  $F_Y(y)$ . Then, the  $\alpha$ -quantile of  $Y$ ,  $q_\alpha$  is defined as

$$q_\alpha = F_Y^{-1}(\alpha)$$

provided that  $F_Y$  is strictly increasing; a similar definition holds in general. The  $\alpha$ -superquantile, denoted by  $\bar{q}_\alpha$ , is defined as the average value of  $Y$  beyond  $q_\alpha$ , i.e.,<sup>3</sup>

$$\bar{q}_\alpha = q_\alpha + \frac{1}{1-\alpha} \mathbb{E}[\max\{Y - q_\alpha, 0\}].$$

Finally, the buffered failure probability  $\bar{p}_f$  of the event  $Y > 0$  is defined as

$$\bar{p}_f = 1 - \bar{\alpha}_0,$$

where  $\bar{\alpha}_0$  is the probability that gives a zero superquantile, i.e.,  $\bar{q}_{\bar{\alpha}_0} = 0$ .

These definitions motivate the shift from the RBO problem (3) to the problem

$$\min_{\mathbf{x} \in \mathbb{X}} c(\mathbf{x}) \tag{7a}$$

$$\text{subject to } \bar{p}(\mathbf{x}) \leq \bar{p}_f^t, \tag{7b}$$

where  $\bar{p}(\mathbf{x})$  is the buffered failure probability of the event  $g_{\text{sys}}(\mathbf{x}, \mathbf{V}) > 0$  and  $\bar{p}_f^t$  is a threshold. This formulation facilitates handling a data-driven setting with  $\mathbf{V}$  replaced by the outcomes  $\mathbf{v}_1, \dots, \mathbf{v}_N$ . In this case, (7) can be reformulated as

$$\min_{\mathbf{x} \in \mathbb{X}, \gamma \in \mathbb{R}} c(\mathbf{x}) \tag{8a}$$

$$\text{subject to } \gamma + \frac{1}{\bar{p}_f^t} \sum_{n=1}^N p_n \max\{0, g_{\text{sys}}(\mathbf{x}, \mathbf{v}_n) - \gamma\} \leq 0, \tag{8b}$$

where  $\gamma$  is an additional real-valued design variable, which at optimality specifies the  $(1 - \bar{p}_f^t)$ -quantile value of  $g_{\text{sys}}(\mathbf{x}, \mathbf{V})$ . It is noted that since  $\gamma$  appears in a well-structured manner, it does not increase computational

---

<sup>3</sup>If  $Y$  is continuously distributed, then  $\bar{q}_\alpha$  is equivalent to the conditional mean  $\mathbb{E}[Y|Y \geq q_\alpha]$ .

complexity. The complexity is also not affected by the maximum operation in the constraint (8b) as the optimization can be reformulated to retain convexity and/or smoothness of the functions within the curly brackets (detailed illustrations can be found in [16]). Accordingly, optimization complexity is governed by  $c(\mathbf{x})$ ,  $g_{\text{sys}}(\mathbf{x}, \mathbf{v}_n)$ , and sample size  $N$ . For instance, if these functions are convex and  $\mathbb{X}$  is a convex set, the problem becomes convex and is thus easily solvable using standard algorithms should  $N$  be of moderate size. In such a convex setting, if instead  $N$  is too large (say  $N \geq 10^4$ ), then the problem can be efficiently solved by nonlinearly-constrained convex bundle methods such as the one proposed in [25]. Even when the functions are neither linear nor convex, the gradients of component limit-state functions  $g_q(\mathbf{x}, \mathbf{v}_n)$  can be used for optimization algorithms, which greatly facilitates implementation as we see below.

In contrast to [17] and its focus on component reliability, we now focus on system reliability. This issue is addressed in this study.

### 2.3. DC programming and DC proximal bundle method in a nutshell

#### 2.3.1. DC programming

The workhorse of our approach is an optimization algorithm capable of efficiently dealing with subproblems of the form

$$\min_{\mathbf{z} \in \mathbb{Z}} f_1(\mathbf{z}) - f_2(\mathbf{z}), \quad (9)$$

where  $f_i : \mathbb{R}^D \rightarrow \mathbb{R}$ ,  $i = 1, 2$ , are nonsmooth convex functions and  $\mathbb{Z} \subset \mathbb{R}^D$  is a simple convex set. To ease the presentation, we assume in this section that  $\mathbb{Z}$  is a polyhedron. Since function  $f(\cdot) = f_1(\cdot) - f_2(\cdot)$  is expressible as the Difference-of-Convex (DC) functions, problem (9) is called a DC program. This family of programs covers a broad class of nonconvex optimization problems but still allows the use of the convex analysis apparatus to establish optimality conditions and design algorithms. However, as DC functions are in general nonconvex, DC programs are NP-hard. We refer to [23, Part II] for a comprehensive presentation of several algorithms that solve DC programs globally and to [26] for a tutorial on DC programming, including the main properties of DC functions, optimality conditions, and local-solution algorithms; see also [14, Ch. 6].

Due to the problem's NP-hardness, it may be difficult to compute a globally optimal solution of (9), let alone proving that an obtained point is globally optimal. Therefore, we will content ourselves with a local-solution algorithm that guarantees convergence to critical points. A point  $\bar{\mathbf{z}} \in \mathbb{Z}$  is said to be critical for problem (9) if

$$\mathbf{0} \in \partial[f_1(\bar{\mathbf{z}}) + i_{\mathbb{Z}}(\bar{\mathbf{z}})] - \partial f_2(\bar{\mathbf{z}}), \quad (10)$$

where  $i_{\mathbb{Z}}(\cdot)$  is the indicator function of the convex set  $\mathbb{Z}$  and, for a convex function  $\varphi : \mathbb{R}^D \rightarrow \mathbb{R}$ , the set<sup>4</sup>  $\partial\varphi(\mathbf{x}) := \{\mathbf{s} : \mathbb{R}^D : \varphi(\mathbf{z}) \geq \varphi(\mathbf{x}) + \langle \mathbf{s}, \mathbf{z} - \mathbf{x} \rangle \text{ for all } \mathbf{z} \in \mathbb{R}^D\}$  is the subdifferential (from convex analysis)

---

<sup>4</sup>Here,  $\langle \mathbf{z}, \mathbf{x} \rangle$  indicates the inner product of two vectors, i.e.,  $\mathbf{z}^T \mathbf{x}$ .

of  $\varphi$  at  $\mathbf{x}$ . It is known that every (local) solution  $\bar{\mathbf{z}}$  of (9) satisfies (10); see for instance [26, § 3]. A simple method for computing critical points for DC programs is the well known DC algorithm [27] that, given an initial point  $\mathbf{z}^1 \in \mathcal{Z}$ , defines iterates as follows:

$$\text{for } \ell = 1, 2, \dots, \text{ compute } \mathbf{s}^\ell \in \partial f_2(\mathbf{z}^\ell) \text{ and define } \mathbf{z}^{\ell+1} \in \arg \min_{\mathbf{z} \in \mathcal{Z}} f_1(\mathbf{z}) - \langle \mathbf{s}^\ell, \mathbf{z} \rangle. \quad (\text{DCA})$$

Although being convex, the above subproblem defining the next iterate can be challenging if  $f_1$  is only known through an oracle (black-box). To overcome this difficulty, [22] proposes to replace such a (potentially complex) convex subproblem with one (or more) strongly convex quadratic programs (QPs).

### 2.3.2. DC proximal bundle method

Instead of defining subproblems featuring the exact function  $f_1$ , the DC bundle method of [22] uses cutting-plane models for both  $f_1$  and  $f_2$ . The main (and mild) assumption is the existence of oracles for  $f_1$  and  $f_2$  providing, for any given  $\mathbf{z}$ , the information  $f_1(\mathbf{z}), \mathbf{s}_1 \in \partial f_1(\mathbf{z})$ , and  $f_2(\mathbf{z}), \mathbf{s}_2 \in \partial f_2(\mathbf{z})$ . Here, the subgradients  $\mathbf{s}_1$  and  $\mathbf{s}_2$  can be arbitrary ones. Having collected bundles  $B_1^\ell, B_2^\ell \subset \{1, 2, \dots, \ell\}$  of oracle information, the method approximates  $f_1$  and  $f_2$  by the cutting-plane models

$$\check{f}_i^\ell(\mathbf{z}) := \max_{j \in B_i^\ell} \{f_i(\mathbf{z}^j) + \langle \mathbf{s}_i^j, \mathbf{z} - \mathbf{z}^j \rangle\} \leq f_i(\mathbf{z}) \quad \forall \mathbf{z} \in \mathbb{R}^D, \quad i = 1, 2.$$

The inequality above follows from convexity. However, the DC cutting-plane model  $\check{f}_1^\ell(\cdot) - \check{f}_2^\ell(\cdot)$  is not necessarily a lower approximation to  $f(\cdot) = f_1(\cdot) - f_2(\cdot)$ , as the example of Figure 1 shows.

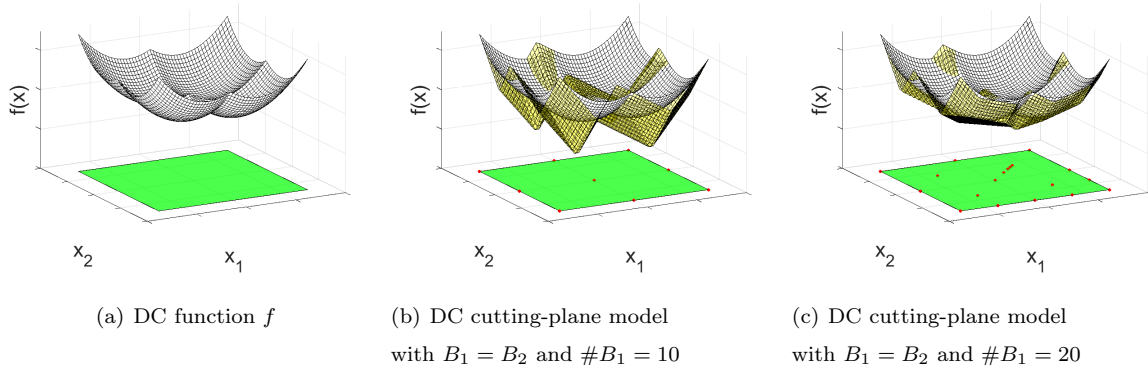


Figure 1. DC model illustration: function  $f$ , pictured in gray, is the DC function  $f(\mathbf{z}) = 1 + \|\mathbf{z}\|^2 - [2|z_1 - 0.1| + 2|z_2 + 0.1|]$ . The DC cutting-plane model is pictured in yellow in subfigures (b) and (c). The dots in red represent the points  $\mathbf{z}^j$  at which both DC component functions  $f_1$  and  $f_2$  are evaluated by the oracles. The notation  $\#B$  stands for the cardinality of set  $B$ .

At every iteration  $\ell$ , the DC bundle method of [22] employs the model  $\check{f}_1^\ell(\cdot) - \check{f}_2^\ell(\cdot)$  and keeps track of the best solution candidate computed so far:  $\hat{\mathbf{z}}^\ell \in \{\mathbf{z}^1, \dots, \mathbf{z}^\ell\}$ . Such a point is termed the method's stability center, as its goal is to keep iterates in its proximity. Mathematically, at iteration  $\ell$ , the method defines the

next iterate by solving the following subproblem, with  $\mu_\ell > 0$  a prox-parameter that is updated by simple rules (e.g.,  $\mu_\ell = \mu > 0$  for all iterations):

$$\mathbf{z}^{\ell+1} \in \arg \min_{\mathbf{z} \in \mathbb{Z}} \check{f}_1^\ell(\mathbf{z}) - \check{f}_2^\ell(\mathbf{z}) + \frac{\mu_\ell}{2} \|\mathbf{z} - \hat{\mathbf{z}}^\ell\|^2. \quad (11)$$

This subproblem is a DC program and becomes a strongly convex QP provided that the index set  $B_2^\ell$  has a single element. Algorithm 1 in [22] is presented with the choice  $\#B_2^\ell = 1$ , where  $\#B$  stands for cardinality of set  $B$ ; however, as explained in Section 4.4, other possibilities are conceivable. Convergence analysis tells us that any choice for  $B_2^\ell$  satisfying  $\hat{\ell} \in B_2^\ell \subset \{1, 2, \dots, \ell\}$  is possible. Here,  $\hat{\ell}$  is the iteration index yielding the stability center, i.e.,  $\hat{\mathbf{z}}^\ell = \mathbf{z}^{\hat{\ell}}$ . Even when  $\#B_2^\ell > 1$ , the above DC subproblem can be globally solved by QP solvers since the definition of  $\check{f}_2^\ell$  yields the following relation

$$\begin{aligned} \min_{\mathbf{z} \in \mathbb{Z}} \check{f}_1^\ell(\mathbf{z}) - \check{f}_2^\ell(\mathbf{z}) + \frac{\mu_\ell}{2} \|\mathbf{z} - \mathbf{z}^\ell\|^2 &= \min_{\mathbf{z} \in \mathbb{Z}} \check{f}_1^\ell(\mathbf{z}) - \max_{j \in B_2^\ell} [f_2(\mathbf{z}^j) + \langle \mathbf{s}_2^j, \mathbf{z} - \mathbf{z}^j \rangle] + \frac{\mu_\ell}{2} \|\mathbf{z} - \mathbf{z}^\ell\|^2 \\ &= \min_{j \in B_2^\ell} \min_{\mathbf{z} \in \mathbb{Z}} \check{f}_1^\ell(\mathbf{z}) - [f_2(\mathbf{z}^j) + \langle \mathbf{s}_2^j, \mathbf{z} - \mathbf{z}^j \rangle] + \frac{\mu_\ell}{2} \|\mathbf{z} - \mathbf{z}^\ell\|^2 \\ &= \min_{j \in B_2^\ell} \left\{ \begin{array}{ll} \min_{\mathbf{z} \in \mathbb{Z}, w \in \mathbb{R}} & w - [f_2(\mathbf{z}^j) + \langle \mathbf{s}_2^j, \mathbf{z} - \mathbf{z}^j \rangle] + \frac{\mu_\ell}{2} \|\mathbf{z} - \mathbf{z}^\ell\|^2 \\ \text{s.t.} & f_1(\mathbf{z}^i) + \langle \mathbf{s}_1^i, \mathbf{z} - \mathbf{z}^i \rangle \leq w \quad \forall i \in B_1^\ell. \end{array} \right. \end{aligned}$$

Hence, globally solving (11) amounts to solve  $\#B_2^\ell$  strongly convex QPs. The computational complexity for defining iterates is thus driven by the decision vector's dimension and size of bundles  $B_1^\ell$  and  $B_2^\ell$ . Fortunately, as shown in [22], the size of the bundle  $B_1^\ell$  (respectively  $B_2^\ell$ ) can be kept as small as 3 (respectively 1) for all iterations  $\ell$  without impairing convergence.

Once the next iterate is defined, the following rule decides when to update the stability center: for  $\kappa \in (0, 1)$  a given parameter,

$$\text{set } \hat{\mathbf{z}}^{\ell+1} = \mathbf{z}^{\ell+1} \text{ if } f(\mathbf{z}^{\ell+1}) \leq f(\hat{\mathbf{z}}^\ell) - \kappa \|\mathbf{z}^{\ell+1} - \hat{\mathbf{z}}^\ell\|^2; \text{ otherwise } \hat{\mathbf{z}}^{\ell+1} = \hat{\mathbf{z}}^\ell. \quad (12)$$

Given a tolerance  $\text{tol} > 0$ , the method stops with an approximate critical point  $\hat{\mathbf{z}}^\ell$  of (9) when the difference  $\|\mathbf{z}^{\ell+1} - \hat{\mathbf{z}}^\ell\| \leq \text{tol}$ . If  $\text{tol} = 0$  and the method stops, then  $\hat{\mathbf{z}}^\ell$  is indeed an exact critical point.

In general lines, the DC proximal bundle algorithm of [22] works as follows.

#### DC Bundle Algorithm:

**Data** Given an initial point  $\mathbf{z}^1 \in \mathbb{Z}$ , set  $\hat{\mathbf{z}}^1 = \mathbf{z}^1$ ,  $B_1^1 = B_2^1 = \{1\}$  and  $\ell = 1$ .

**Step 1** Compute  $\mathbf{z}^{\ell+1}$  by solving (11) and call the oracles at this point.

**Step 2** Stop if  $\|\mathbf{z}^{\ell+1} - \hat{\mathbf{z}}^\ell\| \leq \text{tol}$ .

**Step 3** Update the stability center according to rule (12).

**Step 4** Update the bundles  $B_i^\ell$  by  $B_i^{\ell+1}$ ,  $i = 1, 2$ .

**Step 5** Set  $\ell = \ell + 1$  and go Step 1.

We refer the interested reader to [22, Alg. 1 and § 4.4] for a detailed discussion of every step of the above scheme. Next, we show how to derive DC subproblems of the form (9) that locally approximate the buffered optimization problem (8).

### 3. Proposed reliability-based optimization of general system events: S-BORM algorithm

#### 3.1. Key ideas

To develop an efficient optimization scheme that can handle general systems, we introduce three ideas. First, for optimization, the reliability constraint is penalized and limit-state functions are linearized adaptively at a current candidate solution. Second, by leveraging such linearizations, we derive a DC decomposition of the resulting penalized function that defines a DC program of the form (9). Thereby, we can employ the DC bundle algorithm discussed in the previous section to enhance optimization efficiency and define trial points that are potential candidate solutions to (8). Third, computational efficiency is further improved by employing an active-set strategy. That is, at each iteration of optimization, the algorithm considers only a subset of samples that are within or close enough to failure domains at a current solution, i.e., the samples with the highest limit-state function values. Since the number of failure events are in general very small, this strategy greatly facilitates optimization. More details about active-set strategies are available in [17].

In summary, we solve the complex nonsmooth and nonconvex optimization problem (8) by combining penalization, active-set, and DC techniques. Our approach follows the standard path consisting of replacing a difficult problem with a sequence of simpler subproblems/models. However, our pathway is distinguished from what is largely considered in the optimization literature: invariably, the simpler optimization models have straightforward solutions or are frequently linear/quadratic/convex optimization problems for which efficient solvers exist. In such a way, one is sacrificing model fidelity for computational ease. In this work, we avoid simplistic convex models and locally approximate (8) by tractable nonconvex and nonsmooth optimization subproblems. In pursuing this endeavor, the advantage is that the models' foundation and the link to the original problem are well established, as only the least simplifications necessary to have an implementable approach are engaged. The disadvantage is that subproblems are still challenging and require specialized solvers tailored to their nonconvexity structure. Fortunately, when we linearize the limit-state function in (8) at a given point, we get (thanks to the max-min expressions in (2)) a DC model for the buffered probability function and thus a DC optimization subproblem that modern nonconvex bundle methods can efficiently handle [22].

We name the proposed algorithm *S-BORM* algorithm as it is designed to handle system events. Details of the algorithm are described in following subsections. Section 3.2 derives a DC decomposition in order to apply a proximal bundle method. Thereby, Section 3.3 presents the S-BORM algorithm, which is provided

without a convergence analysis. Therefore, at this stage, the algorithm should be understood as a heuristic. However, some issues related to convergence are briefly discussed in Section 3.4.

### 3.2. Derivation of DC decomposition

To derive the proposed DC decomposition, we introduce mild conditions on a basic constraint set  $\mathbb{X}$  and a cost function  $c(\mathbf{x})$ :  $\mathbb{X} \subset \mathbb{R}^D$  is a polyhedral set, and  $c: \mathbb{R}^D \rightarrow \mathbb{R}$  is a smooth function having  $L$ -Lipschitz continuous gradients over  $\mathbb{X}$ . These conditions should hold for most practical problems. It is noted that convexity is not assumed for either cost function or limit-state functions.

By combining (2) and (8), the optimization problem is constructed as follows:

$$\min_{\mathbf{x} \in \mathbb{X}, \gamma \in \mathbb{R}} c(\mathbf{x}) \quad (13a)$$

$$\text{subject to} \quad \gamma + \frac{1}{\bar{p}_f^t} \sum_{n=1}^N p_n \max\{0, \max_{k \in \{1, \dots, K\}} \min_{q \in \mathbb{Q}_k} g_q(\mathbf{x}, \mathbf{v}_n) - \gamma\} \leq 0, \quad (13b)$$

Then, we penalize the reliability constraint: for  $\theta \in (0, \infty)$ , the optimization problem becomes

$$\min_{\mathbf{x} \in \mathbb{X}, \gamma \in \mathbb{R}} F(\mathbf{x}, \gamma; \theta), \quad \text{with} \quad F(\mathbf{x}, \gamma; \theta) := c(\mathbf{x}) + \theta \max\left\{0, \gamma + \frac{1}{\bar{p}_f^t} \sum_{n \in \hat{\mathbb{N}}} p_n \max\left\{0, \max_{k \in \{1, \dots, K\}} \min_{q \in \mathbb{Q}_k} g_q(\mathbf{x}, \mathbf{v}_n) - \gamma\right\}\right\}. \quad (14)$$

Above, an active-set strategy is assumed, i.e., the problem considers only active samples  $\mathbf{v}_n$  with  $n \in \hat{\mathbb{N}} \subset \{1, \dots, N\}$ . The problem is further approximated by linearizing  $g_q(\mathbf{x}, \mathbf{v}_n)$ ,  $q \in \mathbb{Q}_k$ ,  $k = 1, \dots, K$ , at a candidate solution  $\hat{\mathbf{x}}$ :

$$\min_{\mathbf{x} \in \mathbb{X}, \gamma \in \mathbb{R}} c(\mathbf{x}) + \theta \max\left\{0, \gamma + \frac{1}{\bar{p}_f^t} \sum_{n \in \hat{\mathbb{N}}} p_n \max\left\{0, \max_{k \in \{1, \dots, K\}} \min_{q \in \mathbb{Q}_k} g_q(\hat{\mathbf{x}}, \mathbf{v}_n) + \langle \nabla g_q(\hat{\mathbf{x}}, \mathbf{v}_n), \mathbf{x} - \hat{\mathbf{x}} \rangle - \gamma\right\}\right\}. \quad (15)$$

We now derive a DC decomposition of the objective function of (15) so that we can write the latter as a DC program. To this end, at an iteration step  $\nu$ , consider a current point  $\hat{\mathbf{x}}^\nu$  and a penalization constant  $\theta^\nu$ . Then, the objective function becomes

$$F_\nu^M(\mathbf{x}, \gamma; \theta^\nu, \hat{\mathbf{x}}^\nu) := c(\mathbf{x}) + \theta^\nu \max\left\{0, \gamma + \frac{1}{\bar{p}_f^t} \sum_{n \in \hat{\mathbb{N}}^\nu} p_n \max\left\{0, \max_{k \in \{1, \dots, K\}} \min_{q \in \mathbb{Q}_k} \beta_q^\nu(\mathbf{v}_n) + \langle \alpha_q^\nu(\mathbf{v}_n), \mathbf{x} \rangle - \gamma\right\}\right\}, \quad (16)$$

where  $\hat{\mathbb{N}}^\nu$  is the index set of active samples at step  $\nu$ , and

$$\begin{aligned} \alpha_q^\nu(\mathbf{v}) &= \nabla g_q(\hat{\mathbf{x}}^\nu, \mathbf{v}), \\ \beta_q^\nu(\mathbf{v}) &= g_q(\hat{\mathbf{x}}^\nu, \mathbf{v}) - \langle \nabla g_q(\hat{\mathbf{x}}^\nu, \mathbf{v}), \hat{\mathbf{x}}^\nu \rangle. \end{aligned}$$

The last term of (16) can be decomposed as

$$\begin{aligned} \min_{q \in \mathbb{Q}_k} [\beta_q^\nu(\mathbf{v}) + \langle \alpha_q^\nu(\mathbf{v}), \mathbf{x} \rangle] - \gamma &= \sum_{q \in \mathbb{Q}_k} [\beta_q^\nu(\mathbf{v}) + \langle \alpha_q^\nu(\mathbf{v}), \mathbf{x} \rangle] - \gamma - \max_{q \in \mathbb{Q}_k} \sum_{r \in \mathbb{Q}_k \setminus \{q\}} [\beta_r^\nu(\mathbf{v}) + \langle \alpha_r^\nu(\mathbf{v}), \mathbf{x} \rangle] \\ &:= -p_k^\nu(\mathbf{x}, \gamma, \mathbf{v}). \end{aligned} \quad (17)$$

Since the first and second terms in (17) are linear and convex functions, respectively, we have a convex function

$$p_k^\nu(\mathbf{x}, \gamma, \mathbf{v}) = \max_{q \in \mathbb{Q}_k} \left\{ \sum_{r \in \mathbb{Q}_k \setminus \{q\}} [\beta_r^\nu(\mathbf{v}) + \langle \alpha_r^\nu(\mathbf{v}), \mathbf{x} \rangle] \right\} - \sum_{q \in \mathbb{Q}_k} [\beta_q^\nu(\mathbf{v}) + \langle \alpha_q^\nu(\mathbf{v}), \mathbf{x} \rangle] + \gamma. \quad (18)$$

Let  $q^*$  be an index yielding the maximum in (18). Then, a subgradient of  $p_k^\nu$  at  $(\mathbf{x}, \gamma)$  can be computed as

$$g_{p_k}^\nu(\mathbf{v}) := \begin{pmatrix} \sum_{r \in \mathbb{Q}_k \setminus \{q^*\}} \alpha_r^\nu(\mathbf{v}) - \sum_{q \in \mathbb{Q}_k} \alpha_q^\nu(\mathbf{v}) \\ 1 \end{pmatrix} = \begin{pmatrix} -\alpha_{q^*}^\nu(\mathbf{v}) \\ 1 \end{pmatrix}. \quad (19)$$

We now move on to the next decomposition, i.e.,

$$\begin{aligned} \max_{k=1, \dots, K} \min_{q \in \mathbb{Q}_k} \beta_q^\nu(\mathbf{v}) + \langle \alpha_q^\nu(\mathbf{v}), \mathbf{x} \rangle &= \max_{k=1, \dots, K} -p_k^\nu(\mathbf{x}, \gamma, \mathbf{v}) \\ &= \max_{k=1, \dots, K} \sum_{l \neq k} p_l^\nu(\mathbf{x}, \gamma, \mathbf{v}) - \sum_{k=1}^K p_k^\nu(\mathbf{x}, \gamma, \mathbf{v}) \\ &= \psi^\nu(\mathbf{x}, \gamma, \mathbf{v}) - \varphi^\nu(\mathbf{x}, \gamma, \mathbf{v}), \end{aligned}$$

where both  $\psi^\nu(\mathbf{x}, \gamma, \mathbf{v})$  and  $\varphi^\nu(\mathbf{x}, \gamma, \mathbf{v})$  are convex. Let  $k^*$  be an index yielding the maximum above. Then,

$$g_\varphi^\nu(\mathbf{v}) := \left( \sum_{k=1}^K g_{p_k}^\nu(\mathbf{v}) \right) \in \partial \varphi^\nu(\mathbf{x}, \gamma, \mathbf{v}), \quad \text{and} \quad g_\psi^\nu(\mathbf{v}) := [g_\varphi^\nu(\mathbf{v}) - g_{p_{k^*}}^\nu(\mathbf{v})] \in \partial \psi^\nu(\mathbf{x}, \gamma, \mathbf{v}).$$

Since  $\max\{0, \psi^\nu(\mathbf{x}, \gamma, \mathbf{v}) - \varphi^\nu(\mathbf{x}, \gamma, \mathbf{v})\} = \max\{\psi^\nu(\mathbf{x}, \gamma, \mathbf{v}), \varphi^\nu(\mathbf{x}, \gamma, \mathbf{v})\} - \varphi^\nu(\mathbf{x}, \gamma, \mathbf{v})$ , we can write

$$\begin{aligned} &\gamma + \frac{1}{\bar{p}_f^t} \sum_{n \in \hat{\mathbb{N}}^\nu} p_n \max \left\{ 0, \max_{k \in 1, \dots, K} \min_{q \in \mathbb{Q}_k} \beta_q^\nu(\mathbf{v}_n) + \langle \alpha_q^\nu(\mathbf{v}_n), \mathbf{x} \rangle - \gamma \right\} \\ &= \gamma + \frac{1}{\bar{p}_f^t} \sum_{n \in \hat{\mathbb{N}}^\nu} p_n \left\{ \max \{ \psi^\nu(\mathbf{x}, \gamma, \mathbf{v}_n), \varphi^\nu(\mathbf{x}, \gamma, \mathbf{v}_n) \} - \varphi^\nu(\mathbf{x}, \gamma, \mathbf{v}_n) \right\} \\ &= \gamma + \frac{1}{\bar{p}_f^t} \sum_{n \in \hat{\mathbb{N}}^\nu} p_n \max \{ \psi^\nu(\mathbf{x}, \gamma, \mathbf{v}_n), \varphi^\nu(\mathbf{x}, \gamma, \mathbf{v}_n) \} - \frac{1}{\bar{p}_f^t} \sum_{n=1}^N p_n \varphi^\nu(\mathbf{x}, \gamma, \mathbf{v}_n) \\ &= \Gamma^\nu(\mathbf{x}, \gamma) - \Lambda^\nu(\mathbf{x}, \gamma), \end{aligned}$$

which decomposes into two convex functions

$$\begin{aligned} \Gamma^\nu(\mathbf{x}, \gamma) &= \gamma + \frac{1}{\bar{p}_f^t} \sum_{n \in \hat{\mathbb{N}}^\nu} p_n \max \{ \psi^\nu(\mathbf{x}, \gamma, \mathbf{v}_n), \varphi^\nu(\mathbf{x}, \gamma, \mathbf{v}_n) \}, \\ \Lambda^\nu(\mathbf{x}, \gamma) &= \frac{1}{\bar{p}_f^t} \sum_{n \in \hat{\mathbb{N}}^\nu} p_n \varphi^\nu(\mathbf{x}, \gamma, \mathbf{v}_n). \end{aligned}$$

Their subgradients at  $(\mathbf{x}, \gamma)$  can be computed as

$$g_\Gamma^\nu = \begin{pmatrix} \mathbf{0}_{D \times 1} \\ 1 \end{pmatrix} + \frac{1}{\bar{p}_f^t} \left[ \sum_{n \in \mathbb{N}_x^\psi} p_n g_\psi^\nu(\mathbf{v}_n) + \sum_{n \in \hat{\mathbb{N}}^\nu \setminus \mathbb{N}_x^\psi} p_n g_\varphi^\nu(\mathbf{v}_n) \right], \quad (20a)$$

$$g_\Lambda^\nu = \frac{1}{\bar{p}_f^t} \left[ \sum_{n=1}^N p_n g_\varphi^\nu(\mathbf{v}_n) \right], \quad (20b)$$

where  $\mathbb{N}_x^{\psi, \nu} = \{n \in \hat{\mathbb{N}}^\nu : \psi^\nu(\mathbf{x}, \gamma, \mathbf{v}_n) \geq \varphi^\nu(\mathbf{x}, \gamma, \mathbf{v}_n)\}$ .

Finally, recall that  $c(\mathbf{x})$  has  $L$ -Lipschitz continuous gradients over  $\mathbb{X}$ . Thus,  $c(\mathbf{x}) + \frac{L}{2}\|\mathbf{x}\|^2$  is convex and yields the following DC decomposition for  $c$ :  $c(\mathbf{x}) = c(\mathbf{x}) + \frac{L}{2}\|\mathbf{x}\|^2 - \frac{L}{2}\|\mathbf{x}\|^2$ . Furthermore, by writing  $\max\{0, \Gamma^\nu(\mathbf{x}, \gamma) - \Lambda^\nu(\mathbf{x}, \gamma)\} = \max\{\Gamma^\nu(\mathbf{x}, \gamma), \Lambda^\nu(\mathbf{x}, \gamma)\} - \Lambda^\nu(\mathbf{x}, \gamma)$ , the approximated objective function (16) becomes

$$\begin{aligned} F_\nu^M(\mathbf{x}, \gamma; \theta^\nu, \hat{\mathbf{x}}^\nu) &= c(\mathbf{x}) + \theta^\nu \max\{\Gamma^\nu(\mathbf{x}, \gamma), \Lambda^\nu(\mathbf{x}, \gamma)\} - \theta^\nu \Lambda^\nu(\mathbf{x}, \gamma) \\ &= c(\mathbf{x}) + \frac{L}{2}\|\mathbf{x}\|^2 + \theta^\nu \max\{\Gamma^\nu(\mathbf{x}, \gamma), \Lambda^\nu(\mathbf{x}, \gamma)\} - \left[\frac{L}{2}\|\mathbf{x}\|^2 + \theta^\nu \Lambda^\nu(\mathbf{x}, \gamma)\right] \\ &= f_1^\nu(\mathbf{x}, \gamma) - f_2^\nu(\mathbf{x}, \gamma), \end{aligned} \quad (21a)$$

where

$$f_1^\nu(\mathbf{x}, \gamma) = c(\mathbf{x}) + \frac{L}{2}\|\mathbf{x}\|^2 + \theta^\nu \max\{\Gamma^\nu(\mathbf{x}, \gamma), \Lambda^\nu(\mathbf{x}, \gamma)\}, \quad (21b)$$

$$f_2^\nu(\mathbf{x}, \gamma) = \frac{L}{2}\|\mathbf{x}\|^2 + \theta^\nu \Lambda^\nu(\mathbf{x}, \gamma), \quad (21c)$$

and  $f_1^\nu(\mathbf{x}, \gamma)$  and  $f_2^\nu(\mathbf{x}, \gamma)$  are convex functions with a straightforward rule for computing a pair of subgradients. Hence, we have shown that problem (15) is a DC program of the form (9) with available oracles for the DC component functions. To see that, take in (9)  $\mathbf{z} = (\mathbf{x}, \gamma)$ ,  $\mathbb{Z} = \mathbb{X} \times \mathbb{R}$ , and the above DC decomposition for the objective of (15). Observe that the derived DC decomposition uses the Lipschitz constant  $L$  of the function  $c$ , a value that may be unknown to the decision-maker. However, as  $c(\mathbf{x}) + \frac{\bar{L}}{2}\|\mathbf{x}\|^2$  is still convex for all  $\bar{L} \geq L$  [26, Prop.1], we only need a rough overestimation of this constant to obtain a DC decomposition  $c(\mathbf{x}) + \frac{\bar{L}}{2}\|\mathbf{x}\|^2 - \frac{\bar{L}}{2}\|\mathbf{x}\|^2$  for  $c$ , and thus (in view of (21)) for the objective function of (15). We mention that when  $c$  is convex (the case in our numerical experiments), we can simply set  $\bar{L} = 0$  in (21) and the resulting DC decomposition is still valid.

### 3.3. S-BORM algorithm

Based on the derivation in Section 3.2, we now present the S-BORM algorithm. The algorithm defines iterates as critical points of DC programs using the DC proximal bundle method of [22, Alg. 1] briefly described in Section 2.3.

#### S-BORM Algorithm:

**Data** Given an initial point  $\mathbf{x}^0 \in \mathbb{X}$ , samples  $\{\mathbf{v}_1, \dots, \mathbf{v}_N\}$ , and a parameter  $\gamma^0$ , choose algorithm parameters  $\theta > 0$ ,  $\lambda > 0$ ,  $\omega \geq 1$ ,  $\kappa \in (0, 1)$ , and  $\text{tol}$ .

**Step 0** Set  $\nu = 0$  and  $\hat{\mathbf{x}}^\nu = \mathbf{x}^0$ ,  $\hat{\gamma}^\nu = \gamma^0$ ,  $\theta^\nu = \theta$ ,  $\lambda^\nu = \lambda$ .

**Step 1** Evaluate  $g_{\text{sys}}(\mathbf{x}^\nu, \mathbf{v}_1), \dots, g_{\text{sys}}(\mathbf{x}^\nu, \mathbf{v}_N)$  and obtain an index set of active samples,  $\hat{\mathbb{N}}^\nu \subset \{1, \dots, N\}$ , with the  $\lceil \omega N \bar{p}_f^t \rceil$  greatest values of  $g_{\text{sys}}(\mathbf{x}^\nu, \mathbf{v}_n)$ .

**Step 2** Compute  $\alpha_q^\nu(\mathbf{v}_n) = \nabla g_q(\hat{\mathbf{x}}^\nu, \mathbf{v}_n)$  and  $\beta_q^\nu(\mathbf{v}_n) = g_q(\hat{\mathbf{x}}^\nu, \mathbf{v}_n) - \langle \nabla g_q(\hat{\mathbf{x}}^\nu, \mathbf{v}_n), \hat{\mathbf{x}}^\nu \rangle$  for all  $q \in \mathbb{Q}_k$ ,  $k = 1, \dots, K$  and  $n \in \hat{\mathbb{N}}^\nu$ .

**Step 3** Define  $F_\nu^M(\mathbf{x}, \gamma; \theta^\nu, \hat{\mathbf{x}}^\nu)$  as in (16) and use its DC decomposition (21) to define

$$\min_{\mathbf{x} \in \mathbb{X}, \gamma \in \mathbb{R}} F_\nu^M(\mathbf{x}, \gamma; \theta^\nu, \hat{\mathbf{x}}^\nu) + \frac{\lambda^\nu}{2} \|\mathbf{x} - \hat{\mathbf{x}}^\nu\|_2^2 + \frac{\lambda^\nu}{2} (\gamma - \hat{\gamma}^\nu)^2. \quad (22)$$

Compute a critical point  $(\mathbf{x}^{\nu+1}, \gamma^{\nu+1})$  of this DC subproblem (in our implementation, we used [22, Alg. 1] with initial point  $(\hat{\mathbf{x}}^\nu, \hat{\gamma}^\nu)$ ). If  $\|\mathbf{x}^{\nu+1} - \hat{\mathbf{x}}^\nu\|_2^2 + (\gamma^{\nu+1} - \hat{\gamma}^\nu)^2 \leq \text{tol}$ , stop and return  $(\hat{\mathbf{x}}^\nu, \hat{\gamma}^\nu)$  as a potential solution. Else, go to **Step 4**.

**Step 4** With the penalized function  $F(\cdot, \cdot; \theta^\nu)$  from (14), define the predicted decrease as

$$\zeta^\nu := F(\hat{\mathbf{x}}^\nu, \hat{\gamma}^\nu; \theta^\nu) - F_\nu^M(\mathbf{x}^{\nu+1}, \gamma^{\nu+1}; \theta^\nu, \hat{\mathbf{x}}^\nu) - \frac{\lambda^\nu}{2} \|\mathbf{x}^{\nu+1} - \hat{\mathbf{x}}^\nu\|_2^2 - \frac{\lambda^\nu}{2} (\gamma^{\nu+1} - \hat{\gamma}^\nu)^2.$$

If  $F(\mathbf{x}^{\nu+1}, \gamma^{\nu+1}; \theta^\nu) \leq F(\hat{\mathbf{x}}^\nu, \hat{\gamma}^\nu; \theta^\nu) - \kappa \zeta^\nu$ , declare a **Serious Step**:

$$(\hat{\mathbf{x}}^{\nu+1}, \hat{\gamma}^{\nu+1}) := (\mathbf{x}^{\nu+1}, \gamma^{\nu+1}) \quad \text{and} \quad \lambda^{\nu+1} := \lambda^\nu.$$

Else, declare a **Null Step**:

$$(\hat{\mathbf{x}}^{\nu+1}, \hat{\gamma}^{\nu+1}) := (\hat{\mathbf{x}}^\nu, \hat{\gamma}^\nu) \quad \text{and} \quad \lambda^{\nu+1} := 2\lambda^\nu.$$

**Step 5** Set  $\theta^{\nu+1} := \min\{1.5\theta^\nu, \theta^{\max}\}$ . Replace  $\nu$  by  $\nu + 1$  and go to **Step 1** if Serious Step or **Step 3** if Null Step.

The procedure of the algorithm is as follows. **Step 1** evaluates limit-state functions with a current candidate solution  $\hat{\mathbf{x}}^\nu$  and sorts out active samples  $\hat{\mathbb{N}}$ . Since there are  $N\bar{p}_f^t$  samples of system failure when a reliability constraint is satisfied, the size of  $\hat{\mathbb{N}}$  is set as  $\lceil \omega N\bar{p}_f^t \rceil$  with a parameter  $\omega \geq 1$ . Then, in **Step 2**, the limit-state functions in the penalized problem (14) is linearized to define a DC program. **Step 3** defines the next iterate as a critical point of such DC subproblem. If the new iterate is close enough to a current candidate solution, the algorithm is terminated. Otherwise, in **Step 4**, a descent test *à la* bundle method is carried out. If the new iterates leads to satisfactory decrease in the objective function, this update is considered a Serious Step: the new iterate becomes the current candidate solution. Otherwise, it is a Null Step: the candidate solution does not change, and its prox-parameter  $\lambda^\nu$  is increased to force the next iterate to be closer to the best computed point so far. At the end of each iteration, in **Step 5**,  $\theta^\nu$ , which penalizes violating reliability constraints is increased (as standard in penalization approaches). Thereby, solutions can be gradually nudged towards feasible regions, i.e., feasibility with respect to reliability constraints.

The proposed algorithm has three major parameters: the two penalty terms  $\lambda$  and  $\theta$  and the ratio of active samples,  $\omega$ . The default values of these parameters are proposed as  $\lambda_0 = 0.01$ ,  $\theta_0 = 1$ ,  $\theta^{\max} = 10^5$  and

$\omega = 2$ , which are also used in the following examples. Other minor parameters are  $\kappa$  and `tol`.  $\kappa$  decides the criterion whether to accept a new candidate solution. `tol` is the stopping threshold of Euclidean distance between the candidate solution and the new iterate. Default values of both parameters are proposed as 0.01. It is noted that these parameters have little influence on optimization results as demonstrated by numerical examples in Section 4. In Section 5, we further demonstrate robustness of the proposed algorithm by performing parametric study under various settings.

### 3.4. Algorithm justification

As already mentioned, the S-BORM algorithm should be understood as a heuristic, as we do not provide a complete convergence analysis. However, in what follows, we justify why our approach makes sense.

First, observe that the descent test in **Step 4** is a valid one provided that the predicted decrease  $\zeta^\nu$  is non-negative. This will be certainly the case if we apply a monotone decreasing DC method to (22) with initial point  $(\hat{\mathbf{x}}^\nu, \hat{\gamma}^\nu)$ , justifying thus (in addition to the hard-to-evaluate objective function) our suggestion of using [22, Alg. 1]. Indeed, note that the model evaluated at the current candidate solution coincides with the function value at this point, i.e.,

$$F_\nu^M(\hat{\mathbf{x}}^\nu, \gamma; \theta^\nu, \hat{\mathbf{x}}^\nu) = F(\hat{\mathbf{x}}^\nu, \gamma; \theta^\nu), \quad \forall \gamma.$$

Therefore, since  $(\hat{\mathbf{x}}^\nu, \hat{\gamma}^\nu)$  is feasible to the subproblem of **Step 3**, we have that

$$F_\nu^M(\mathbf{x}^{\nu+1}, \gamma^{\nu+1}; \theta^\nu, \hat{\mathbf{x}}^\nu) + \frac{\lambda^\nu}{2} \|\mathbf{x}^{\nu+1} - \hat{\mathbf{x}}^\nu\|_2^2 + \frac{\lambda^\nu}{2} (\gamma^{\nu+1} - \hat{\gamma}^\nu)^2 \leq F_\nu^M(\hat{\mathbf{x}}^\nu, \hat{\gamma}^\nu; \theta^\nu, \hat{\mathbf{x}}^\nu).$$

As the right-hand side coincides with  $F(\hat{\mathbf{x}}^\nu, \hat{\gamma}^\nu; \theta^\nu)$ , we conclude that the predicted decrease  $\zeta^\nu$  is non-negative and S-BORM is a descent method (provided that the penalization parameter is fixed).

Now, observe that since  $(\mathbf{x}^{\nu+1}, \gamma^{\nu+1})$  is a critical point of (22), with  $F_\nu^M(\mathbf{x}, \gamma; \theta^\nu, \hat{\mathbf{x}}^\nu)$  decomposed as  $f_1^\nu(\mathbf{x}, \gamma) - f_2^\nu(\mathbf{x}, \gamma)$  given in (21), we conclude that

$$\mathbf{0} \in \partial[f_1^\nu(\mathbf{x}^{\nu+1}, \gamma^{\nu+1}) + i_{\mathbb{X}}(\mathbf{x}^{\nu+1})] + \lambda^\nu \begin{pmatrix} \mathbf{x}^{\nu+1} - \hat{\mathbf{x}}^\nu \\ \gamma^{\nu+1} - \hat{\gamma}^\nu \end{pmatrix} - \partial f_2^\nu(\mathbf{x}^{\nu+1}, \gamma^{\nu+1}), \quad \forall \nu = 1, 2, \dots \quad (23)$$

Hence, if at certain iteration  $\nu$ , **Step 3** produces  $(\mathbf{x}^{\nu+1}, \gamma^{\nu+1}) = (\hat{\mathbf{x}}^\nu, \hat{\gamma}^\nu)$ , the above inclusion becomes

$$\mathbf{0} \in \partial[f_1^\nu(\hat{\mathbf{x}}^\nu, \hat{\gamma}^\nu) + i_{\mathbb{X}}(\hat{\mathbf{x}}^\nu)] - \partial f_2^\nu(\hat{\mathbf{x}}^\nu, \hat{\gamma}^\nu),$$

showing that  $(\hat{\mathbf{x}}^\nu, \hat{\gamma}^\nu)$  is a critical point for the penalized/linearized problem (15) (with  $\theta = \theta^\nu$  and  $\hat{\mathbf{x}} = \hat{\mathbf{x}}^\nu$ ).

Next, we argue that a similar conclusion also follows in an asymptotic analysis. Since iterates in our algorithm can be of two types, the asymptotic analysis of S-BORM should be split into two parts, depending on whether the serious step sequence is finite or infinite. By assuming `tol` = 0 and that the S-BORM algorithm loops indefinitely, let us first comment on the first case.

The algorithm produces only finitely many serious steps followed by an infinite sequence of null steps. In this case, the current stability center is fixed for all iterations large enough:

$$(\hat{\mathbf{x}}^\nu, \hat{\gamma}^\nu) = (\hat{\mathbf{x}}, \hat{\gamma}) \quad \text{for all } \nu \geq \hat{\nu}, \quad (24)$$

with  $\hat{\nu}$  the iteration index of the last serious step. Furthermore, the linearization of limit-state functions are fixed for these iterations, and thanks to **Step 3** the S-BORM algorithm boils down to a penalized approach for the DC program

$$\min_{\mathbf{x} \in \mathbf{X}, \gamma \in \mathbb{R}} c(\mathbf{x}) \quad (25a)$$

$$\text{subject to} \quad \gamma + \frac{1}{\bar{p}_f^t} \sum_{n=1}^N p_n \max \left\{ 0, \max_{k \in \{1, \dots, K\}} \min_{q \in \mathbb{Q}_k} g_q(\hat{\mathbf{x}}, \mathbf{v}_n) + \langle \nabla g_q(\hat{\mathbf{x}}, \mathbf{v}_n), \mathbf{x} - \hat{\mathbf{x}} \rangle - \gamma \right\} \leq 0. \quad (25b)$$

To see this, compare (15) and (25). Furthermore, as the penalized parameter becomes  $\theta^{\max}$  after finitely many steps, the iterates produced by **Step 3** converges to  $(\hat{\mathbf{x}}, \hat{\gamma})$  as  $\lambda^\nu$  increases indefinitely and the value  $F_\nu^M(\mathbf{x}, \gamma; \theta^{\max}, \hat{\mathbf{x}})$  given in (16) does not change (because both the penalization parameter and the current solution candidate are fixed for all  $\nu$  large enough). This argument, together with (23),  $\|\mathbf{x}^{\nu+1} - \hat{\mathbf{x}}^\nu\|_2^2 + (\gamma^{\nu+1} - \hat{\gamma}^\nu)^2 \rightarrow 0$  and (24), suggests that  $(\hat{\mathbf{x}}, \hat{\gamma})$  is a critical point for the linearized problem, i.e.,

$$\mathbf{0} \in \partial[f_1^\nu(\hat{\mathbf{x}}, \hat{\gamma}) + i_{\mathbf{X}}(\hat{\mathbf{x}})] - \partial f_2^\nu(\hat{\mathbf{x}}, \hat{\gamma}).$$

The theory of exact penalty functions asserts that if a condition on the constraint of (25) exists, and  $\theta^{\max}$  is greater than the largest optimal dual variable associated with this constraint, then solutions of the penalized problem (15) are solutions of (25); see [28] and [29].

The algorithm produces infinitely many serious steps. Again, recall that penalized parameter becomes  $\theta^{\max}$  after finitely many iterations. In this case, as already argued, the descent test ensures that the sequence of function values is non-increasing:

$$F(\hat{\mathbf{x}}^{\nu+1}, \hat{\gamma}^{\nu+1}; \theta^{\max}) \leq F(\hat{\mathbf{x}}^\nu, \hat{\gamma}^\nu; \theta^{\max}) - \kappa \zeta^\nu, \quad \text{with } \zeta^\nu \text{ given in Step 4.}$$

With the mild assumption that  $F(\cdot, \cdot; \theta^{\max})$  has bounded level sets, a simple recursive argument (the telescope sum) on the above inequality shows that  $\zeta^\nu \rightarrow 0$  and, once again,  $\|\mathbf{x}^{\nu+1} - \hat{\mathbf{x}}^\nu\|_2^2 + (\gamma^{\nu+1} - \hat{\gamma}^\nu)^2 \rightarrow 0$ . By combining these results with (23), we can argue that any cluster point  $(\bar{\mathbf{x}}, \bar{\gamma}^\nu)$  of the sequence of serious steps  $\{(\hat{\mathbf{x}}^\nu, \hat{\gamma}^\nu)\}$  is critical for the penalized problem (15) with  $\hat{\mathbf{x}}$  replaced with  $\bar{\mathbf{x}}$ . Once again, the penalization arguments concerning (15) and (25) apply.

*Summary.* The above arguments tell us that the S-BORM algorithm always terminates after finitely many steps provided that  $\text{tol} > 0$ . When  $\text{tol} = 0$ , the discussion on the asymptotic behaviour of the algorithm

suggests<sup>5</sup> us that the approach computes a critical point for the linearized problem (25), with  $\hat{x}$  being the  $x$ -part of the last serious step, or an arbitrary cluster point (if any) of  $\{\hat{x}^\nu\}$ . The main issue with a complete convergence analysis for our approach is the link, in terms of optimality conditions, between the linearized problem (15) (or (25)) and the original buffered failure probability problem (8): what does a critical point for the linearized problem represent for the original one? The answer is simple if the limit-state variables are linear, as in the first example of our numerical experiments: in this case, the two problems coincide, and thus S-BORM computes a critical point for the buffered failure probability problem. Answering the above question in the more general setting of this work is left as a future research direction.

We finalize this section by mentioning that for the quest of computing a global solution for problem (8), we may rely on the computational efficiency of our approach (empirically demonstrated in Section 5.3) and try multiple initializations: being a nonsmooth and nonconvex optimization problem, the quality of a candidate solution provided by any local-solution algorithm depends on the initial point.

## 4. Numerical examples

### 4.1. Experiment settings

Algorithm parameters are set as the default values proposed in Section 3.3. On the other hand, for all problems, initial solutions are set as the midpoint of upper and lower bounds of design variables. The target buffered failure probability is  $\bar{p}_f^t = 10^{-3}$ , and the target coefficient of variance (c.o.v.) is  $\delta^t = 0.05$ . This leads to the number of samples,  $(1 - \bar{p}_f^t)/(\bar{p}_f^t \cdot (\delta^t)^2) = 399,600$ . Then, with the default parameter  $\omega = 2$ , the number of active samples becomes  $\lceil 2 \cdot 399,600 \cdot 10^{-3} \rceil = 800$ .

### 4.2. Design of cantilever beam-bar system

This example investigates an optimal design of a cantilever beam-bar system illustrated in Figure 2. The system consists of an ideally plastic cantilever beam of moment capacity  $M$  and length  $2L = 2 \cdot 5$ , which is propped by an ideally rigid-brittle bar of strength  $T$  [30]. The structure is subjected to load  $P$  that is applied on the middle of the bar. Load  $P$  is a random variable following the normal distribution with mean  $\mu_P = 150$  and standard deviation  $\sigma_P = 30$ . Moment  $M$  and strength  $T$  are also normal random variables with mean  $\mu_M$  and  $\mu_T$  and standard deviation  $\sigma_M = 300$  and  $\sigma_T = 20$ , respectively. In this example, we optimize two design variables  $x_1 = \mu_M \in [500, 1500]$  and  $x_2 = \mu_T \in [50, 150]$ . The cost function is  $c(x) = 2x_1 + x_2$ .

---

<sup>5</sup>The above is a mere discussion, not a mathematical proof.

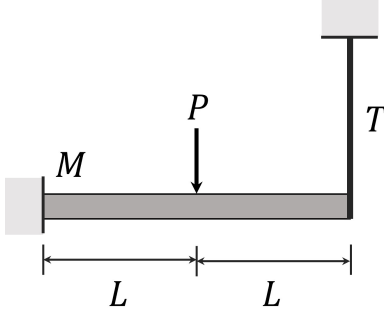


Figure 2. Example cantilever beam-bar system (figure recreated from Song and Der Kureghian [30])

Song and Der Kureghian [30] identified six limit-state functions such that

$$\begin{aligned}
 g_1(\mathbf{x}, \mathbf{v}) &= -(x_2 + v_2 - 5v_3/16), \\
 g_2(\mathbf{x}, \mathbf{v}) &= -(x_1 + v_1 - Lv_3), \\
 g_3(\mathbf{x}, \mathbf{v}) &= -(x_1 + v_1 - 3Lv_3/8), \\
 g_4(\mathbf{x}, \mathbf{v}) &= -(x_1 + v_1 - Lv_3/3), \\
 g_5(\mathbf{x}, \mathbf{v}) &= -(x_1 + v_1 + 2L \cdot (x_2 + v_2) - Lv_3),
 \end{aligned}$$

where  $v_1$  and  $v_2$  are a realization of the normal distribution with zero mean and standard deviation  $\sigma_M$  and  $\sigma_T$ , respectively; and  $v_3$  is a realization of  $P$ . The system event consists of three cut-sets such that  $E_{\text{system}} = E_1E_2 \cup E_3E_4 \cup E_3E_5$ .

With the S-BORM algorithm, the computed solution is  $(x_1, x_2) = (150.0, 1, 297)$ , resulting in estimated buffered failure probability  $\hat{p}_f = 9.985 \cdot 10^{-4}$  and cost 2,743. For comparison, a grid search is performed by discretizing each variable into 100 intervals, which leads to 1.01 and 10.1 spacing for  $x_1$  and  $x_2$ , respectively. The search identifies the best point as (149.0, 1, 298) leading to cost 2,745,  $\hat{p}_f = 9.935 \cdot 10^{-4}$ , and  $\hat{p}_f = 2.678 \cdot 10^{-4}$ . This agrees with the solution computed by the proposed algorithm. The optimization requires a marginal computational efforts taking 0.136 seconds. It runs 7 outer loops and 7 rounds of gradient evaluations of the samples, which implies that only 7 evaluations of limit-state functions are made for each sample and 7 gradient evaluations are made for each active sample. The summary of the results can be found in Table 1.

#### 4.3. Design of indeterminate truss bridge system

Consider a truss bridge structure in Figure 3. The structure consists of 10 members with strength  $R_i$ ,  $i = 1, \dots, 10$ , which are independent normal random variables with mean  $\mu_R = 276$  and standard deviation  $\sigma_R = 13.8$ . The parameters of member lengths are set as  $H = 1.6$  and  $L = 2$ . The truss structure is subjected to load  $P$  exerted on nodes 1 and 2, which follows the normal distribution with mean  $\mu_P = 190$

and standard deviation  $\sigma_P = 19$ . Then, the design variables are cross-section areas of the members. To reflect the practical aspect of construction, the members are grouped into four sets such that  $\{1, 2, 9, 10\}$ ,  $\{3, 8\}$ ,  $\{4, 7\}$ , and  $\{5, 6\}$ . Within a group, members have the same cross-section area, which is represented by a design variable  $x_1, x_2, x_3$ , and  $x_4$  in order, where  $x_d \in [1, 2]$ ,  $d = 1, \dots, 4$ . The cost function is the total volume of the members, i.e.,  $c(\mathbf{x}) = \sum_{q=1}^{10} l_q \cdot x_{d(q)}$ , where  $l_q$  is the length of member  $q$ , and  $d(q)$  denotes the index of the group that member  $q$  belongs to, e.g.,  $d(1) = 1$  and  $d(3) = 2$ .

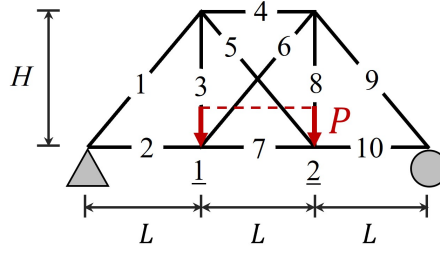


Figure 3. Example truss structure system

The system failure is defined as an occurrence of structural instability. Such occurrence can be identified by performing structural analysis. Each failure mode, i.e., a sequence of member failures that leads to a system failure, can be represented as a cut-set, whereby the system event is defined as a link-set of those cut-sets. For example, as a failure of member 1 incurs structural instability, member 1 constitutes a cut-set. Another example is a failure of member 3 followed by that of member 7. Such failure of member  $q$  at failure mode  $k$  can be represented by a limit-state function

$$g_{kq}(\mathbf{x}, \mathbf{v}) = v_0 \cdot \delta_{kq} - x_{d(q)} \cdot v_q,$$

where  $v_0$  is a realization of  $P$ ;  $\delta_{kq}$  is the force experienced by member  $q$  in failure mode  $k$  when a unit force is applied to nodes 1 and 2; and  $v_q$ ,  $q = 1, \dots, 10$ , is a realization of  $R_q$ . As 108 failure modes are identified for this structure, the system event becomes

$$E_{\text{sys}} = \bigcup_{k=1}^{108} \bigcap_{q \in Q_k} E_{kq},$$

where  $Q_k$  denotes the index set of members that constitute a failure mode  $k$ .

As summarized in Table 1, an optimal solution is obtained as (1.586, 1.000, 1.459, 1.000) with cost 28.63,  $\hat{p}_f = 9.735 \cdot 10^{-4}$ , and  $\hat{p}_f = 3.654 \cdot 10^{-4}$ . The optimization takes 13.6 seconds with 3 rounds of outer loops and 3 rounds of gradient evaluations.

#### 4.4. Testing time allocation on electrical components

Consider the two transmission-line electrical substation system in Figure 4 [31]. The system consists of 12 components, which either fail or survive. Then, system failure is defined as a disconnection between

the input and output nodes. Each component type is under a test phase, and we aim to find an optimal allocation of testing time over the component types. There are 6 component types, i.e., disconnect switch (DS), circuit breaker (CB), power transformer (PT), drawout breaker (DB), tie breaker (TB), and feeder breaker (FB), and their testing time is denoted by design variables  $x_1, \dots, x_6$ , respectively. We assume that their reliability growth follows the non-homogeneous Poisson process (NHPP) reliability growth model (RGM) [32], by which the fault rate of component  $q$  of type  $d(q)$ ,  $q = 1, \dots, 12$  is defined as

$$\lambda_j(x_{d(q)}) = \frac{\alpha\beta}{\exp(\beta x_{d(q)})},$$

where the parameters are set as  $\alpha = 9$  and  $\beta = 2$ . The cost function is the total testing time, i.e.,  $c(x) = \sum_{d=1}^4 x_d$ . On the other hand, for each component  $q$ , the limit-state function is defined as

$$\begin{aligned} g_j(x_{d(q)}, v_q) &= \Delta T - \frac{-\ln v_q}{\lambda_q(x_{d(q)})} \\ &= \Delta T + \ln v_q \cdot \frac{\exp(\beta x_{d(q)})}{\alpha\beta}, \end{aligned}$$

where  $\Delta T = 365$  is the target operation time, and  $\xi_q$ ,  $q = 1, \dots, 12$ , is a realization of the uniform distribution  $U[0, 1]$ . The system consists of 25 minimum cut sets  $\{(1, 2), (4, 5), (4, 7), (4, 9), (5, 6), (6, 7), (6, 9), (5, 8), (7, 8), (8, 9), (11, 12), (1, 3, 5), (1, 3, 7), (1, 3, 9), (2, 3, 4), (2, 3, 6), (2, 3, 8), (4, 10, 12), (6, 10, 12), (8, 10, 12), (5, 10, 11), (7, 10, 11), (9, 10, 11), (1, 3, 10, 12), (2, 3, 10, 11)\}$  [31].

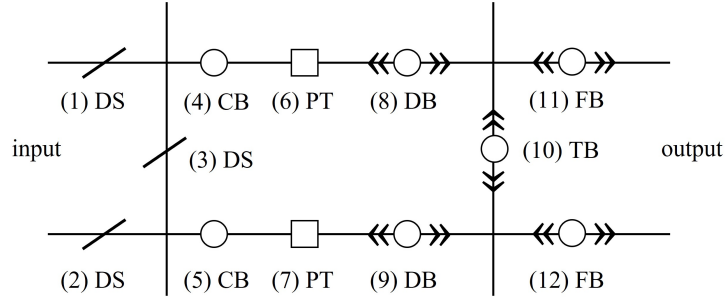


Figure 4. Example electrical system (figure recreated from Der Kureghian et al. [31])

As summarized in Table 1, an optimal solution is computed as  $(7.017, 7.047, 7.095, 7.024, 1.000, 7.016)$  with cost 36.20,  $\hat{p}_f = 9.635 \cdot 10^{-4}$ , and  $\hat{p}_f = 4.179 \cdot 10^{-4}$ . Since all component types are assigned an identical RGM, difference in testing time arises solely from varying topological importance. The optimization takes 2.83 seconds with 10 rounds of evaluations of limit-state functions and 10 rounds of gradient evaluations of active samples.

Ex.	Time (sec.)	No. of outer loops (function calls) <sup>a</sup>	No. of serious steps (gradient calls) <sup>b</sup>	Computed solution	Cost	$\hat{p}_f$ ( $\times 10^{-4}$ )	$\hat{p}_f$ ( $\times 10^{-4}$ )
1	0.136	7 (2,797,200)	7 (5,600)	(150.0, 1,297)	2,743	9.985	2.678
2	13.6	3 (1,198,800)	3 (2,400)	(1.586, 1.000, 1.459, 1.000)	28.63	9.735	3.654
3	2.83	10 (3,996,000)	10 (8,000)	(7.017, 7.047, 7.095, 7.024, 1.000, 7.016)	36.20	9.860	4.429

<sup>a</sup> (No. of outer loops) $\times$ (No. of samples) = (Total evaluation number of limit-state functions)

<sup>b</sup> (No. of serious steps) $\times$ (No. of active samples) = (Total evaluation number of limit-state function gradients)

Table 1. Optimization results of three numerical examples

## 5. Parametric test of the proposed algorithm

### 5.1. Algorithm parameters

While default values of the algorithm parameters are proposed in Section 4.1, we test the robustness of the algorithm by running optimization with their values changed. First, experiments are performed by changing  $\lambda$  to 0.005, 0.02, 0.04, 0.08, and 1. The results are summarized in Table 2. As illustrated in the table, the parameter does not incur notable differences. In all of the three examples, the computation time remains stable taking less than 1 minute. Also, for other results including the number of outer loops and gradient evaluations, cost,  $\hat{p}_f$ , and  $\hat{p}_f$ , highest and lowest values all remain very close. Similarly,  $\theta$  is changed to 0.25, 0.5, 2, 4, and 8. Table 3 summarizes the highest and lowest values of various results. Again, the results do not show notable variances. Finally,  $\omega$  is tested with values 1.2, 1.5, 2, 3, and 5, as illustrated in Table 4. This parameter also does not lead to meaningful differences.

Although the parameters are found to have insignificant influences, there are still marginal variances in computation time and quality of solutions (i.e., the cheapest solution that satisfies reliability constraints). Numerical experiments suggest that the proposed default values show the most stable performance. Nevertheless, one may alter their values to fit the characteristics of a given problem. For example, one may increase  $\lambda$  if solutions are too slow to converge, jumping between distant regions.  $\theta$  can be increased if the algorithm finds it hard to satisfy reliability constraints.  $\omega$  needs to be increased if active sets change wildly as an optimal solution is updated, or decreased if evaluation of limit-state functions is costly.

### 5.2. Target buffered failure probability

To test its stability to the magnitude of target buffered failure probability (i.e.,  $\bar{p}_f^t$ ), the algorithm is tested with target values  $1 \times 10^{-2}$  and  $1 \times 10^{-4}$ . The optimization results are summarized in Table 5. In the

Ex.		Time (sec.)	No. of outer loops	No. of serious steps	Cost	$\hat{\bar{p}}_f$ ( $\times 10^{-4}$ )	$\hat{p}_f$ ( $\times 10^{-4}$ )
1	Highest	0.73 ( $\lambda = 1$ )	26 ( $\lambda = 1$ )	26 ( $\lambda = 1$ )	2,743 ( $\lambda = 0.005$ )	9.985 (all $\lambda$ )	3.103 ( $\lambda = 1$ )
	Lowest	0.14 ( $\lambda = 0.01$ )	7 ( $\lambda = 0.01$ )	7 ( $\lambda = 0.01$ )	2,718 ( $\lambda = 0.04$ )	9.985 (all $\lambda$ )	2.678 ( $\lambda = 0.005$ )
2	Highest	55 ( $\lambda = 1$ )	4 ( $\lambda = 0.05$ )	4 ( $\lambda = 0.05$ )	29.35 ( $\lambda = 0.04$ )	9.760 ( $\lambda = 1$ )	3.754 ( $\lambda = 1$ )
	Lowest	19 ( $\lambda = 0.01$ )	2 ( $\lambda = 1$ )	2 ( $\lambda = 1$ )	28.63 ( $\lambda = 0.01$ )	8.834 ( $\lambda = 0.08$ )	3.353 ( $\lambda = 0.005$ )
3	Highest	4.9 ( $\lambda = 1$ )	10 (all $\lambda$ )	10 (all $\lambda$ )	36.78 ( $\lambda = 1$ )	9.960 ( $\lambda = 0.08$ )	4.354 ( $\lambda = 0.08$ )
	Lowest	2.1 ( $\lambda = 0.08$ )	10 (all $\lambda$ )	10 (all $\lambda$ )	36.14 ( $\lambda = 0.08$ )	9.635 ( $\lambda = 0.04$ )	4.304 ( $\lambda = 0.04$ )

Table 2. Optimization results obtained by different parameters  $\lambda = 0.005, 0.01, 0.02, 0.04, 0.08$ , and 1

Ex.		Time (sec.)	No. of outer loops	No. of serious steps	Cost	$\hat{\bar{p}}_f$ ( $\times 10^{-4}$ )	$\hat{p}_f$ ( $\times 10^{-4}$ )
1	Highest	0.21 ( $\theta = 0.05$ )	12 ( $\theta = 0.25$ )	10 ( $\theta = 0.5$ )	2,743 ( $\theta = 0.25$ )	9.985 (all $\theta$ )	3.128 ( $\theta = 8$ )
	Lowest	0.14 ( $\theta = 1$ )	3 ( $\theta = 4$ )	3 ( $\theta = 4$ )	2,718 ( $\theta = 4$ )	9.985 (all $\theta$ )	2.678 ( $\theta = 0.25$ )
2	Highest	51 ( $\theta = 0.5$ )	4 ( $\theta = 0.25$ )	3 ( $\theta = 8$ )	28.82 ( $\theta = 2$ )	9.960 ( $\theta = 2$ )	3.879 ( $\theta = 2$ )
	Lowest	19 ( $\theta = 1$ )	2 ( $\theta = 2$ )	2 ( $\theta = 2$ )	28.61 ( $\theta = 8$ )	7.432 ( $\theta = 4$ )	2.928 ( $\theta = 4$ )
3	Highest	2.2 ( $\theta = 2$ )	10 (all $\theta$ )	10 (all $\theta$ )	39.21 ( $\theta = 8$ )	9.910 ( $\theta = 2$ )	4.455 ( $\theta = 2$ )
	Lowest	2.1 ( $\theta = 4$ )	10 (all $\theta$ )	10 (all $\theta$ )	36.15 ( $\theta = 4$ )	9.735 ( $\theta = 0.25$ )	4.204 ( $\theta = 0.25$ )

Table 3. Optimization results obtained by different parameters  $\theta = 0.25, 0.5, 1, 2, 4$ , and 8

table, comparisons are made in parentheses with the results in Table 1 with target probability  $1 \times 10^{-3}$ . As expected, in all examples, the cost of obtained solutions increases with a higher  $\bar{p}_f^t$ . It is noted that computing time and the number of iterations remain stable, while the estimated buffered failure probabilities remain close but lower than the target values. This demonstrates the robustness of the algorithm with respect to the level of  $\bar{p}_f^t$ .

Ex.		Time (sec.)	No. of outer loops	No. of serious steps	Cost	$\hat{p}_f$ ( $\times 10^{-4}$ )	$\hat{p}_f$ ( $\times 10^{-4}$ )
1	Highest	0.40 ( $\omega = 5$ )	10 ( $\omega = 1.2$ )	7 ( $\omega = 2$ )	2,743 ( $\omega = 1.2$ )	9.985 (all $\omega$ )	3.05 ( $\omega = 5$ )
	Lowest	0.14 ( $\omega = 1.2$ )	8 ( $\omega = 5$ )	6 ( $\omega = 1.2$ )	2,718 ( $\omega = 3$ )	9.985 (all $\omega$ )	2.678 ( $\omega = 2$ )
2	Highest	42 ( $\omega = 1.2$ )	6 ( $\omega = 1.5$ )	5 ( $\omega = 1.5$ )	29.29 ( $\omega = 3$ )	9.860 ( $\omega = 1.2$ )	3.779 ( $\omega = 1.2$ )
	Lowest	19 ( $\omega = 2$ )	2 ( $\omega = 1.2$ )	2 ( $\omega = 1.2$ )	28.61 ( $\omega = 1.2$ )	8.684 ( $\omega = 1.5$ )	3.353 ( $\omega = 3$ )
3	Highest	5.13 ( $\omega = 5$ )	10 (all $\omega$ )	10 (all $\omega$ )	38.39 ( $\omega = 5$ )	9.860 ( $\omega = 2$ )	4.330 ( $\omega = 2$ )
	Lowest	1.4 ( $\omega = 1.2$ )	10 (all $\omega$ )	10 (all $\omega$ )	36.06 ( $\omega = 1.5$ )	9.585 ( $\omega = 1.5$ )	4.054 ( $\omega = 1.5$ )

Table 4. Optimization results obtained by different parameters  $\omega = 1.2, 1.5, 2, 3$ , and 5

$\bar{p}_f^t = 0.1 \times 10^{-2}$							
Ex.	Time (sec.)	No. of outer loops	No. of serious steps	Computed solution	Cost	$\hat{p}_f$	$\hat{p}_f$
1	0.131 (-0.00527)	8 (+1)	8 (+1)	(150.0, 1,092)	2,334 (-409.3)	9.975 $\times 10^{-3}$	3.030 $\times 10^{-3}$
2	40.4 (+26.8)	2 (-1)	2 (-1)	(1.501, 1.090, 1.338, 1.000)	27.73 (-0.6300)	9.015 $\times 10^{-3}$	3.636 $\times 10^{-3}$
3	3.21 (+0.387)	6 (-4)	6 (-4)	(6.435, 6.435, 6.435, 6.435, 2.218, 6.435)	34.39 (-1.809)	9.949 $\times 10^{-3}$	4.268 $\times 10^{-3}$
$\bar{p}_f^t = 0.1 \times 10^{-4}$							
1	0.561 (+0.425)	7 (+0)	7 (+0)	(150.0, 1,471)	3,091 (+348.2)	9.976 $\times 10^{-5}$	3.100 $\times 10^{-5}$
2	32.8 (+19.2)	3 (+0)	3 (+0)	(1.668, 1.000, 1.765, 1.000)	29.72 (+1.090)	9.801 $\times 10^{-5}$	3.300 $\times 10^{-5}$
3	5.80 (+2.98)	8 (-2)	8 (-2)	(7.615, 7.616, 7.617, 7.616, 1.000, 7.616)	39.08 (+2.881)	9.801 $\times 10^{-5}$	4.350 $\times 10^{-5}$

Table 5. Optimization results obtained by different target values of buffered failure probability (in parentheses, comparisons are made with results in Table 1.)

### 5.3. Initial points

Since problems of interest are non-convex, the quality of computed solutions is most dependent on initial points. To test this, for each example, 100 experiments are performed with different initial points sampled by Latin hypercube sampling. The best solutions of each example, i.e., the solution that satisfies reliability constraints and incur the lowest cost, are summarized in Table 6. By considering a solution the best if it yields a cost less than 3% higher than the lowest obtained value, it is observed that 100%, 46%, and 7% of the initial points lead to one of the best solutions in the first, second, and third examples, respectively. This suggests that the third example has in particular multiple local optima. It is noted that the results in Table 1, which are obtained with initial solutions as a midpoint of the lower and upper bounds, are all one of the best obtained solutions. Nonetheless, the result strongly indicates that one needs to try multiple initializations to ensure the quality of an obtained solution. The proposed algorithm is advantageous to this end owing to its computational efficiency as demonstrated by various tests illustrated above.

Ex.	Best optimal solution <sup>a</sup>	Cost	$\hat{\hat{p}}_f$ ( $\times 10^{-4}$ )	$\hat{p}_f$ ( $\times 10^{-4}$ )	Ratio of best solutions <sup>b</sup>
1	(150.0, 1,257)	2,709	9.960	3.203	100 %
2	(1.581, 1.000, 1.443, 1.000)	28.52	9.835	3.679	46 %
3	(7.215, 6.896, 7.391, 7.391, 1.000, 6.906)	36.80	6.857	3.053	7 %

<sup>a</sup> The feasible solution leading to the lowest cost

<sup>b</sup> Feasible solutions leading to a cost less than 3% higher than the lowest one

Table 6. Optimization results with varying initial solutions

## 6. Conclusions

This study proposes an efficient algorithm for reliability-based optimization (RBO), particularly for general system events that are represented as a link-set of cut-sets. To handle such general systems, we evaluate system reliability by realizations of random variables (i.e., samples or data points) instead of analytical calculation that requires problem-specific formulas. This can be done by employing the buffered optimization and reliability method (BORM) that replaces the conventional failure probability by the buffered failure probability. We call it the *S-BORM* algorithm.

The S-BORM algorithm efficiently solves RBO problems of general systems by leveraging three ideas. First, it linearizes the limit-state functions at a current solution and iteratively solves a resulting subproblem until solutions converge. Second, such linearization enables us to derive a DC decomposition of RBO

problems and thereby, employ a proximal bundle method for optimization. Third, the algorithm makes use of an active-set strategy, whereby it can consider only a small subset of samples that are within or close enough to failure domains. We do not assume convexity either for cost function or for limit-state functions. This makes the S-BORM algorithm applicable for a wide class of systems. Although such minimal assumptions make it difficult (if not impossible) to theoretically guarantee global optimality and convergence, we provide justifications of the proposed approach and empirical demonstrations through numerical examples. Examples include complex and large-scale systems such as a truss structure system with 108 failure modes and an electrical system undergoing reliability growth. Moreover, extensive parametric investigations show that the algorithm remains insensitive to algorithm parameter values and magnitude of target failure probability, which further proves its applicability.

Utilizing realizations of random variables greatly facilitates general applications as it eliminates the need for problem-specific derivations and enables non-parametric analysis. By leveraging such advantages, we develop a Matlab-based tool, which is available at <https://github.com/jieunbyun/sborm>. To run the algorithm, users only need to provide general information, i.e., cost functions and limit-state functions (including their gradients) and realizations of random variables. Meanwhile, this indicates a distinct potential of the BORM for further development of general software tools of reliability-based optimization. This is advantageous considering barriers of implementing RBO algorithms, which often require a high level of knowledge and engineering. Promising topics for being combined with such data-driven optimization include surrogate models, real-time data, and sequential decision-making.

## **Acknowledgement**

The first author is supported by the Humboldt Research Fellowship for Postdoctoral Researchers from Alexander von Humboldt Foundation. The second author acknowledges financial support from the Gaspard-Monge Program for Optimization and Operations Research (PGMO) project “SOLEM - Scalable Optimization for Learning and Energy Management”. The research of the third author is supported in part by the Air Force Office of Scientific Research, Mathematical Optimization (21RT0484).

## **Conflicts of interest**

The authors have no relevant financial or non-financial interests to disclose.

## **Replication of results**

The examples can be replicated by (Matlab-based) codes and data uploaded at <https://github.com/jieunbyun/sborm>.

## References

- [1] I. Enevoldsen, J. D. Sørensen, Reliability-based optimization in structural engineering, *Structural Safety* 15 (1994) 169–196.
- [2] J.-E. Byun, J. Song, Efficient probabilistic multi-objective optimization of complex systems using matrix-based bayesian network, *Reliability Engineering and System Safety* 200 (2020) 106899.
- [3] J.-E. Byun, J. Song, A general framework of bayesian network for system reliability analysis using junction tree, *Reliability Engineering and System Safety* 216 (2021) 107952.
- [4] H.-W. Lim, J. Song, Efficient risk assessment of lifeline networks under spatially correlated ground motions using selective recursive decomposition algorithm, *Earthquake Engineering and Structural Dynamics* 41 (2012) 1861–1882.
- [5] T. H. Nguyen, J. Song, G. H. Paulino, Single-loop system reliability-based topology optimization considering statistical dependence between limit-states, *Structural and Multidisciplinary Optimization* 44 (2011) 593–611.
- [6] J. O. Royset, A. Der Kiureghian, E. Polak, Reliability-based optimal structural design by the decoupling approach, *Reliability Engineering and System Safety* 73 (2001) 213–221.
- [7] E. Bismut, M. D. Pandey, D. Straub, Reliability-based inspection and maintenance planning of a nuclear feeder piping system, *Reliability Engineering and System Safety* 224 (2022) 108521.
- [8] J. Kim, J. Song, Reliability-based design optimization using quantile surrogates by adaptive gaussian process, *ASCE Journal of Engineering Mechanics* 147 (2021) 04021020.
- [9] X. Li, C. Gong, L. Gu, Z. Jing, H. Fang, R. Gao, A reliability-based optimization method using sequential surrogate model and monte carlo simulation, *Structural and Multidisciplinary Optimization* 59 (2019) 439–460.
- [10] P. Perdikaris, D. Venturi, J. O. Royset, G. E. Karniadakis, Multi-fidelity modelling via recursive co-kriging and gaussian–markov random fields, *Proc. R. Soc. A.* 471 (2015) 20150018.
- [11] A. Canelas, M. Carrasco, J. López, A new method for reliability analysis and reliability-based design optimization, *Structural and Multidisciplinary Optimization* 59 (2019) 1655–1671.
- [12] Y. Ding, Y. Hu, D. Li, Redundancy optimization for multi-performance multi-state series-parallel systems considering reliability requirements, *Reliability Engineering and System Safety* 215 (2021) 107873.
- [13] S. Li, X. Chi, B. Yu, An improved particle swarm optimization algorithm for the reliability–redundancy allocation problem with global reliability, *Reliability Engineering and System Safety* 225 (2022) 108604.
- [14] J. O. Royset, R. J.-B. Wets, *An Optimization Primer*, 1 ed., Springer Cham, 2021.
- [15] J. O. Royset, E. Polak, Extensions of stochastic optimization results to problems with system failure probability functions, *Journal of Optimization Theory and Applications* 133 (2007) 1–18.
- [16] R. T. Rockafellar, J. O. Royset, On buffered failure probability in design and optimization of structures, *Reliability Engineering and System Safety* 95 (2010) 499–510.
- [17] J.-E. Byun, J. O. Royset, Data-driven optimization of reliability using buffered failure probability, *Structural Safety* 98 (2022) 102232.
- [18] J. O. Royset, J.-E. Byun, Gradients and subgradients of buffered failure probability, *Operations Research Letters* 49 (2021) 868–873.
- [19] A. Chaudhuri, B. Kramer, M. Norton, J. O. Royset, K. Willcox, Certifiable risk-based engineering design optimization, *AIAA Journal* 60 (2022) 551–565.
- [20] J. Bonnans, J. Gilbert, C. Lemaréchal, C. Sagastizábal, *Numerical Optimization. Theoretical and Practical Aspects*, Universitext, Springer-Verlag, Berlin, 2006. Second edition, xiv+490 pp.
- [21] W. de Oliveira, C. Sagastizábal, Bundle methods in the XXI century: A birds’-eye view, *Pesquisa Operacional* 34 (2014) 647–670.

- [22] W. de Oliveira, Proximal bundle methods for nonsmooth DC programming, *Journal of Global Optimization* 75 (2019) 523–563.
- [23] H. Tuy, *Convex Analysis and Global Optimization*, 2 ed., Springer, 2016.
- [24] W. van Ackooij, S. Demassey, P. Javal, H. Morais, W. de Oliveira, B. Swaminathan, A bundle method for nonsmooth DC programming with application to chance-constrained problems, *Computational Optimization and Applications* 78 (2021) 451–490.
- [25] W. van Ackooij, W. de Oliveira, Level bundle methods for constrained convex optimization with various oracles, *Computational Optimization and Applications* 57 (2014) 555–597.
- [26] W. de Oliveira, The ABC of DC programming, *Set-Valued and Variational Analysis* 28 (2020) 679–706.
- [27] H. A. Le Thi, P. D. Tao, DC programming and DCA: thirty years of developments, *Mathematical Programming* 169 (2018) 5–68.
- [28] S. Han, O. L. Mangasarian, Exact penalty functions in nonlinear programming, *Mathematical Programming* 17 (1979) 251–269.
- [29] H. A. Le Thi, T. Pham Dinh, H. V. Ngai, Exact penalty and error bounds in DC programming, *Journal of Global Optimization* 52 (2012) 509–535.
- [30] J. Song, A. Der Kureghian, Bounds on system reliability by linear programming, *ASCE Journal of Engineering Mechanics* 129 (2003) 627–636.
- [31] A. Der Kureghian, O. D. Ditlevsen, J. Song, Availability, reliability and downtime of systems with repairable components, *Reliability Engineering and System Safety* 92 (2007) 231–242.
- [32] J.-E. Byun, J. Song, Reliability growth analysis of k-out-of-n systems using matrix-based system reliability method, *Reliability Engineering and System Safety* 165 (2017) 410–421.